Geomorphology 184 (2013) 98–110

Contents lists available at SciVerse ScienceDirect

Geomorphology

journal homepage: www.elsevier.com/locate/geomorph

A case of rapid rock riverbed incision in a coseismic uplift reach and its implications

Ming-Wan Huang, Yii-Wen Pan *, Jyh-Jong Liao

Department of Civil Engineering, National Chiao Tung University, 1001, University Road, Hsinchu, 30010, Taiwan

ARTICLE INFO

Article history:
Received 20 June 2012
Received in revised form 21 November 2012
Accepted 26 November 2012
Available online 3 December 2012

Keywords:
Coseismic uplift
Incision rate
Taan River
Chi-Chi earthquake
Taiwan

ABSTRACT

During the 1999 Chi-Chi earthquake ($M_w = 7.6$) in Taiwan, the coseismic displacement induced fault scarps and a pop-up structure in the Taan River. The fault scarps across the river experienced maximum vertical slip of 10 m, which disturbed the dynamic equilibrium of the fluvial system. As a result, rapid incision in the weak bedrock, with a maximum depth of 20 m, was activated within a decade after its armor layer was removed. This case provides an excellent opportunity for closely tracking and recording the progressive evolution of river morphology that is subjected to coseismic uplift. Based on multistaged orthophotographs and digital elevation model (DEM) data, the process of morphology evolution in the uplift reach was divided into four consecutive stages. Plucking is the dominant mechanism of bedrock erosion associated with channel incision and knickpoint migration. The astonishingly high rate of knickpoint retreat (KPR), as rapid as a few hundred meters per year, may be responsible for the rapid incision in the main channel. The reasons for the high rate of KPR are discussed in depth. The total length of the river affected by the coseismic uplift is 5 km: 1 km in the uplift reach and 4 km in the downstream reach. The downstream reach was affected by a reduction in sediment supply and increase in stream power. The KPR cut through the uplift reach within roughly a decade; further significant flooding in the future will mainly cause widening instead of deepening of the channel.

1. Introduction

River morphology is closely associated with the processes of sedimentation and erosion, which react dynamically to external influences such as climatic change, tectonics, isostatic adjustments, and human factors; these processes result in alterations of the landscape (Gilbert, 1877; Schumm, 1979). The evolution study of river morphology usually requires a studied site with long-term and chronologically reforming topographic data to develop proper theories or verify corresponding models (Howard et al., 1994; Tomkin et al., 2003). Among others, the dominant factor affecting landform evolution is the incision rate of the riverbed rock (Whipple, 2004). However, the erosion rate of bedrock is often too slow to trace during a study period; consequently, the process of bedrock erosion is quite difficult to infer from limited data with the exception of the average incision rate. In addition, the scale of time may affect the average incision rate, e.g., the knickpoint migration rate is negatively correlated to the timescale of observation (Loget and Van Den Driessche, 2009). Fundamental data of reaches with erodible bedrocks could facilitate the interpretation of major processes/mechanisms and the development of appropriate models of bedrock erosion.

From the aspect of tectonic-driven deformation, slow uplift tends to induce a progressively small incision in the fluvial system. In contrast, abrupt faulting with significant vertical displacement often exceeds the adjusting threshold of dynamic equilibrium and may initiate rapid morphological changes in a fluvial channel on a corresponding scale. The catastrophic Chi-Chi earthquake ($M_w = 7.6$), which took place in central Taiwan in 1999, caused large-scale casualties and damage in Taiwan. In this earthquake, a surface rupture with a length of 100 km was observed. Thrust faulting generated fault scarps or pop-up type deformations across four main rivers in central Taiwan (including the Taan River, the Tachia River, the Wu River, and the Choshui River). The fault scarps across the rivers experienced maximum vertical slip of 10 m (Lee et al., 2003), which changed the dynamic equilibrium of the local fluvial system and resulted in rapid river incision. In this case, the incident of faulting provides an exceptional opportunity for studying the complete evolution processes of river morphology and bedrock erosion that are caused by the disturbance of faulting.

Yanites et al. (2010a,b) proposed a conceptual model for explaining the evolution process of landforms at the proximal and distal reaches of a fault in response to a coseismic uplift of the fault. They chose the Pei-Kang River (a branch of the Wu River in central Taiwan) as an example. A knickpoint near the fault was generated by the fault scarp and migrated upstream. The vertical incision rate on the knickpoint was significantly higher than the long-term average incision rate. In reaches distal to the fault, the abundant sediment supply from the earthquake-triggered landslides either slowed or halted the riverbed incision. The time to reinitiate downcutting is largely dependent on the sediment transport capacity for removing the landslide material.

To propose the drainage basin evolution, fine-elevation data (e.g., produced by Light Detection and Ranging, LiDAR) and a time-efficient

* Corresponding author. Tel.: +886 3 5712121x54931; fax: +886 3 5716257.
E-mail address: ywpan@mail.nctu.edu.tw (Y.-W. Pan).

0169-555X/$ – see front matter © 2012 Elsevier B.V. All rights reserved.
http://dx.doi.org/10.1016/j.geomorph.2012.11.022

model could be utilized to produce a realistic simulation, e.g., Anders et al. (2009). Nevertheless, the varying channel flow and sediment transport capacity may play an important role in bedrock erosion (Lai et al., 2011). Numerical analyses that adopt two-dimensional mobile-bed models were conducted by Liao et al. (2011) and Lai et al. (2011) for simulations of landform evolution in the Taan River and in the Choshui River, respectively; both rivers are in central Taiwan. Independent incision mechanisms including hydraulic erosion and saltating abrasion were considered in their erosion models. The results of the simulations demonstrated that the channel incision trends were qualitatively equivalent to the observed data. However, to improve the numerical simulation quantitatively, the dynamic evolution process of rock riverbed caused by uplift faulting requires further study.

The coseismic uplift in the Taan River is relatively high among the rivers that encountered surface rupture during the Chi-Chi earthquake in central Taiwan (Lee et al., 2005; Chen et al., 2007). Rapid river bed incision reshaped the original landform from a wide channel in the uplift reach to a gorge-like channel with a maximum depth of 20 m in less than a decade (Huang et al., 2008). The rapidly incised reach was greatly induced by knickpoint migration. The highest local incision rate was 14 m within one flooding season. The maximum rate of knickpoint retreat (KPR) was 350 m during one flooding season, which was even more astonishing (Huang et al., 2012). Because the average rate of bedrock incision in this case was in the order of meters, interpreting the bedrock erosion process on the basis of multistaged orthophotographs and digital elevation model (DEM) data was feasible. Using the uplift reach as an example, this work conducted geological surveys including erosion phenomena observations, analyses and interpretation of multistaged (mostly annually) terrain data, and analyses of discharge data for major flooding events. Beginning with the presentation of background information, we describe and interpret the process of morphology evolution in four consecutive stages. Next, we discuss the observed evolution of landforms, various mechanisms of erosion, characteristics of knickpoint migration, future tendency for erosion, and insights from observations in this study.

2. Background

2.1. Taan River

The Taan River is located in central west Taiwan (Fig. 1A). Its drainage area is 758 km^2 with a trunk length of 96 km. The river headwaters are 3500 m asl from the west wing of the Hsuehshan mountain range. The majority of the basin is in mountainous or hilly areas. The first 60-km trunk from the headwater is confined in a mountainous valley with an elevation higher than 500 m and a channel slope generally steeper than 2% (Fig. 1B). Away from the mountainous area, the channel slope flattens to 1.5% and gradually reduces to < 1% near the estuary. Because of the subtropical climate, the mean annual precipitation in the Taan River is 1800 mm in plain areas, 2500 mm in hilly areas, and even greater in mountainous areas. Nearly three-quarters of rainfall is recorded during the wet season, which occurs from May to October. Typhoons frequently produce concentrated and intense precipitation.

2.2. Effects of the 1999 Chi-Chi earthquake

The Chi-Chi earthquake ($M_w = 7.6$) occurred on 21 September 1999 in central Taiwan; this catastrophic earthquake produced surface ruptures of 100 km in length along the Che-Long-Pu fault. The fault strikes northbound and bends eastbound at its northern end. The surface ruptures terminated after they passed the Taan River valley in the NE–SW direction (Fig. 1A). The northern part of the earthquake ruptures (E–W direction) consisted of a few minor branches; some of the branches followed preexisting geological structures (Lee et al., 2005). Across the Taan River valley, two surface ruptures were parallel to the Tungshih anticline (Fig. 2). The two parallel ruptures were fold scarps associated with the synclinal bends at the base of the two fold limbs of the anticline (Chen et al., 2007). The pop-up structure was part of the Tungshih anticline (Fig. 2) with a longitudinal distance of 1 km and a maximum uplift of 10 m (Fig. 1C).

2.3. Study site

The uplift reach in the Taan River is located between 27.7 and 28.7 km upstream from the estuary (Fig. 1B and C). Before the Chi-Chi earthquake, the average channel slope was 1.3%. After the earthquake, four prominent terrain features were found from downstream to upstream (Fig. 1C and D): (i) the height of the rupture scarp on the downstream side was 5 m; (ii) the average slope of the river channel from the downstream scarp to the fold axis of the Tungshih anticline increased to 5%; (iii) the average slope of the river channel from the fold axis of the Tungshih anticline to the upstream scarp reduced to 0.3%; and (iv) the rupture scarp on the upstream side was 6 m in height; it blocked the river flow by forming a barrier lake that resulted in deposition of sediments in the barrier lake and further flattening of the upstream-channel slope. At the beginning of the uplift (Figs. 1D and 3A, 22 Sep 1999 DEM and aerial orthophotograph), the river in the study reach remained a braided-type channel with a high width/depth ratio. Eleven years later (Figs. 1E and 3B, 12 Sep 2010 DEM and aerial orthophotograph), the river landform became a deeply entrenched channel with a steep rock bank. Most of the river flow concentrated in the main channel. Although a few minor flow routes with limited discharge existed, they could not hold significant flow.

The bedrock exposed in the reach belongs to the Pliocene Cholan Formation. It is composed of sandstone, siltstone, mudstone, and shale in a monotonous alternating sequence. The young sediment rocks are poorly cemented with low erosion resistance. Fig. 2 displays the surface geological map that is based on outcrops and borehole cores. Five sampling boreholes were drilled including four boreholes on the river banks and one borehole on the river channel. The Tungshih anticline is the major geological structure in this site. As noted in the geological cross section, the anticline showed a flat top near the axis that slightly plunged toward the SW direction; the tilted beddings dipped downstream and upstream at two limbs.

2.4. Terrain data

This study utilized three types of topographic data (including data from cross section surveys, derived DEMs from aerial photographs, and airborne LiDAR DEMs) to analyze multistaged terrain changes in this reach. In general, the data from cross section surveys, which was not misled by vegetation shelter and flow body, were more accurate and reliable than the DEM. However, only three cross sections and three periods of surveys (Mar 2003, Mar 2004, and Dec 2007) were available after the earthquake. The data alone was not sufficient for describing the terrain changes. Cross section data were used for verifying the correctness of the DEMs.

Because the studied site was a 1-km-long reach with sparse vegetation, the DEM data were applied directly without further editing. Twelve sets of DEM data for consecutive time periods were utilized for the comparison of terrain changes (Table 1). The DEMs from aerial photographs were derived via a commercial program and a set of field-surveyed ground control points (GCP). Most of the aerial photographs, with an average scale of 1:20,000, were purchased from the Aerial Survey Office of the Forestry Bureau in Taiwan, which has periodically collected aerial photography for land resource surveys since the 1970s. The DEM data and some aerial photographs were obtained from airborne LiDAR. These aerial photographs were also rectified into orthogonal images for visual observation.

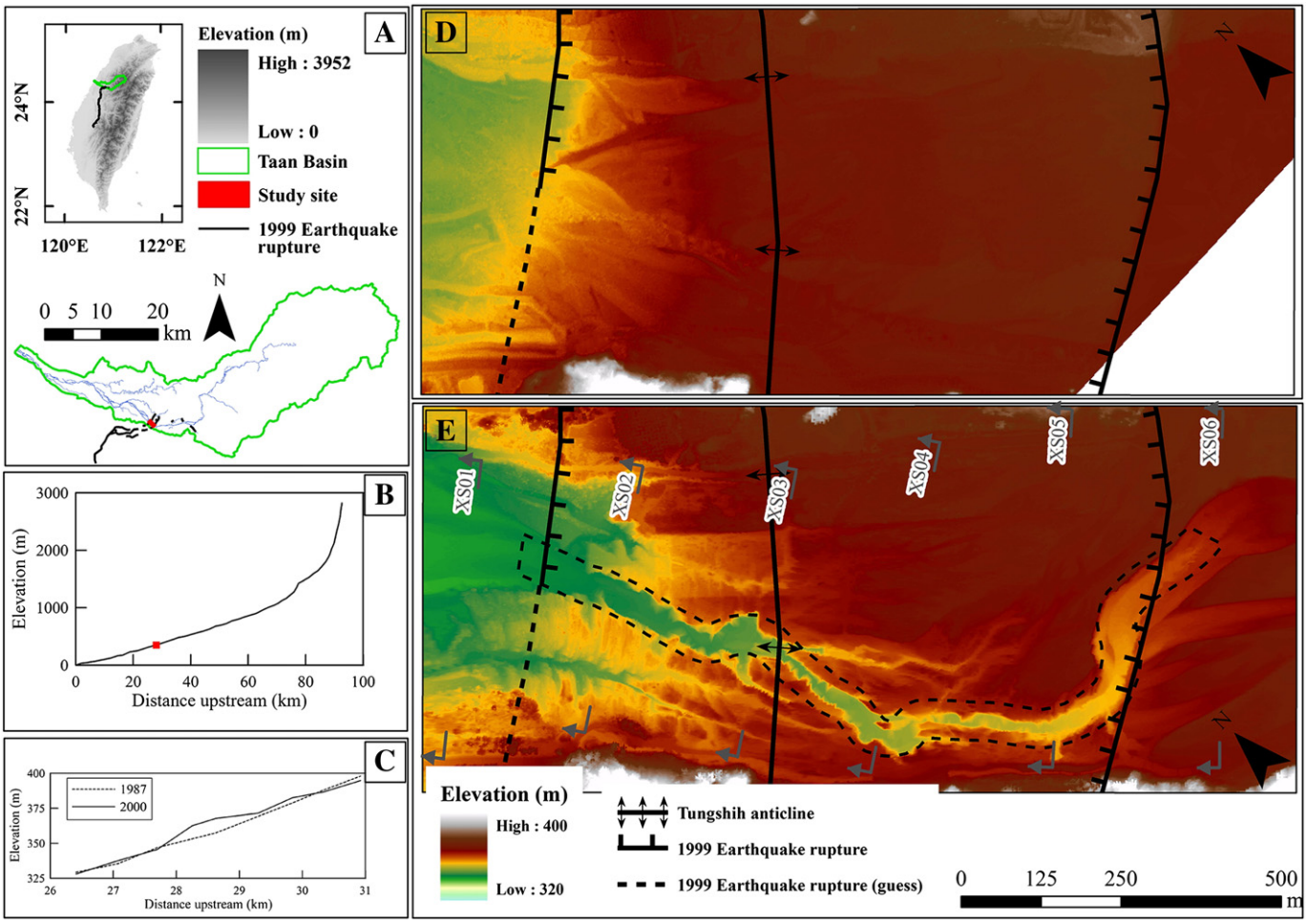

Fig. 1. Overview of the studied area. (A) The location of the studied site is near the northern end of ruptures from the Chi-Chi earthquake. The shaded relief map shows the location of the Taan basin in Taiwan and the rupture lines caused by the earthquake. (B) Longitudinal profile of the Taan River. (C) Comparison of longitudinal profiles near the uplifted reach before and after the earthquake. (D) DEM image derived from aerial photographs on 22 Sep 1999. The studied reach is between the lines (ticks on uplift side) of ruptures. (E) Image of LiDAR survey DEM on 12 Sep 2010. Black-dash polygon indicates the location of the main channel; longitudinal geological profiles in Fig. 5 are analyzed inside the area of main channel. Gray arrows and lines indicate the locations of cross sections analyzed in Fig. 6.

2.5. Discharge data

Originally, a gauging station (Cholan station) was at the Cholan bridge located 2 km downstream of the uplift reach; it malfunctioned after the 1999 Chi-Chi earthquake. To realize the chronological discharge data and precipitation data for the Taan River basin, a kinematic wave-based geomorphologic instantaneous unit hydrograph (KW-GIUH) model (Lee and Yen, 1997) was adopted to estimate the discharge at the Cholan station. Fig. 4 shows the major flood events (with peak discharge >300 m^3/s) for each of the four consecutive morphology stages after the Chi-Chi earthquake. These four morphology stages will be defined in the subsequent section. The largest flood discharge since 1999 was 7364 m^3/s during Typhoon Aere (25 Aug 2004, in Fig. 4, stage 2); this discharge was ~200 times the average daily discharge (36 m^3/s). Fig. 4 also shows the drastic differences in river flow between dry and wet seasons, especially during typhoon seasons. For this reach, the estimated flood discharges corresponding to 2-year, 5-year, and 10-year return periods were ~2690, 4890, and 6640 m^3/s, respectively (WRA, 2010).

3. Distinct stages of morphology evolution

The morphology evolution of the uplift reach was divided into four distinct stages according to landform characteristics. The landform characteristics were identified through field observations and comparisons of terrain data using multistaged orthogonal aerial photographs, longitudinal profiles, and lateral cross sections (Figs. 5 and 6) along the channel. In stage 1 (1999 to 2001), sediment transportable downstream was blocked or cut down because of landform alterations and emergency dredging. In stage 2 (2001 to 2004), along with bedrock exposure, intense incision in the exposed bedrock happened in the downstream area of the anticline axis because of the head difference adjacent to the rupture scarp. In stage 3 (2004 to 2007), after the accumulative incision in the second stage, several bedrock channels were developed and began to compete with each other. The most eroded channel eventually developed into the main channel, which was relatively deeper and wider. Simultaneously, the bedrock on the upstream side of the anticline axis was also gradually exposed, expanded, and subjected to incision. Finally in stage 4 (2007 to 2010), the bedrock incision remained active toward the upstream scarp and eventually carved through the uplift reach along the main channel. Once the main channel ultimately cut through the entire uplift reach, sediment transport downstream was reinitiated; afterward, deposition was observed on the downstream side where channel incision was previously intense. As a result, the slope of the main flow channel gradually approached an equilibrium state.

3.1. Stage 1: 1999 to 2001 loss of armor layer

As mentioned previously, the coseismic ground deformation caused the vicinity of the studied reach to uplift along the preexisting structure

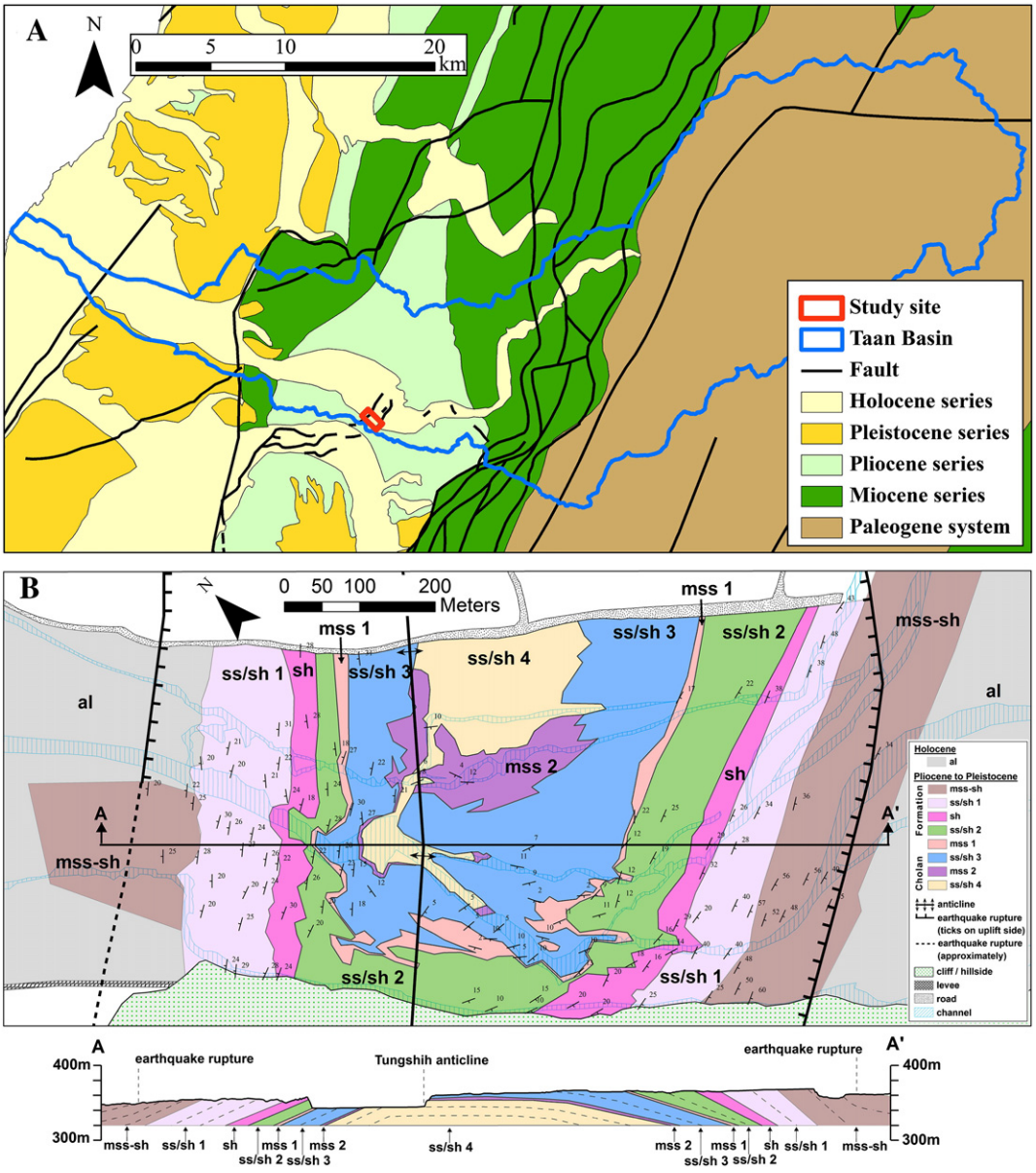

Fig. 2. (A) General geological map of the Taan basin. (B) Geological map of the studied site. The topography is based on the 2009 LiDAR DEM. Abbreviations: mss = massive sandstone; ss = sandstone; sh = shale; ss/sh = thin interlayered shale and sandstone; mss-sh = massive sandstone with occasional thin shale; al = alluvium.

(Tungshih anticline), which produced a pop-up structure across the river. As a result, the river flow was obstructed upstream where a barrier lake formed behind the rupture scarp (Figs. 3A and 5A). After the formation of the barrier lake, an emergency dredging plan was conducted in the uplift reach. Because of the dredging and the sediments trapped in the barrier lake, the armor layer in the uplift reach was quickly lost. Although the barrier lake was potentially harmless, 3–5 m of armor materials was removed. The dredging operation may have greatly accelerated the time of fluvial incision into the bedrock.

In this stage, the major change in the longitudinal profile (Fig. 5A) was the thickness of the armor layer. A few features of the landform change from downstream to upstream are described as follows. In the downstream region of the uplift reach, no clear sign of channel incision was observed (Fig. 6, XS01). In the downstream region of the anticline axis (i.e., the west limb of the anticline), the channel slope increased substantially after the coseismic uplift. The armor layer was completely lost and the exposed bedrock began to erode (Fig. 6, XS02 and 03). In the region between the anticline axis and the upstream rupture, the channel slope decreased after the coseismic uplift; the thin armor material remained visible (Fig. 6, XS04 and 05). In the region inside the barrier lake, the thickness of alluvium gradually increased as a result of sediment deposition in the lake (Fig. 6, XS06).

3.2. Stage 2: 2001 to 2004 intense incision of exposed bedrock

The channel incision progressed from downstream to upstream (Fig. 5B). As a result of bedrock incision with insufficient sediment supply, the elevation of the downstream channel decreased, which enhanced the channel incision on its upstream side. In this stage, intense incision occurred in the downstream region of the anticline axis and two obvious knickpoints appeared (Fig. 5B). The alluvial material, which was originally 10 m in thickness, near section XS01 disappeared (Fig. 6). Several incised channels developed near section XS02 with a maximum incision depth of 10 m (Fig. 6). The entire armor layer was

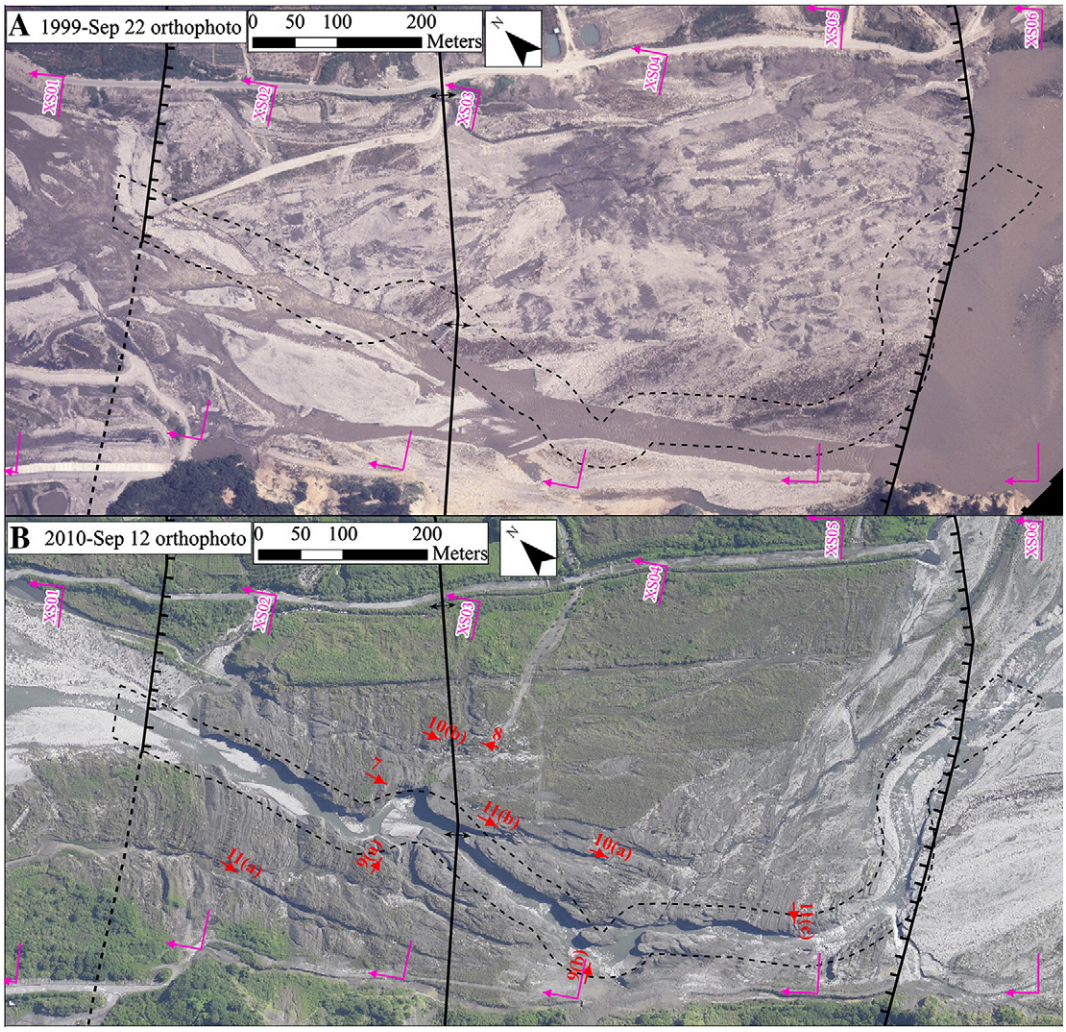

Fig. 3. Aerial orthophotos of the uplift reach: (A) 22 Sep 1999; (B) 12 Sep 2010. Black-dash polygon indicates the location of main channel. Pink arrows and lines indicate the locations of cross sections analyzed in Fig. 6. The red arrow shows the photographing location and direction in Figs. 7 to 11.

almost eroded in the region located upstream of the anticline axis (Fig. 5B). The main channel deflected to the left bank (Fig. 6, XS03, 04, and 05) most likely because the axis of the Tungshih anticline plunged toward the left bank (Fig. 2B). In the region of the barrier lake, the alluvium thickness continued to increase but gradually slowed (Fig. 6, XS06). In general, the bedrock incision in this stage occurred mainly in the downstream side of the anticline axis. Several shallow and narrow incised channels were competed for the final main channel. Bedrock exposure gradually expanded toward the upstream region, which enabled bedrock erosion in that area.

3.3. Stage 3: 2004 to 2007 formation of main channel

Bedrock erosion was much more active than in previous stages because of the concentrated discharge in the main channel and the effect of knickpoint migration. The maximum incision in the main channel was >10 m (Fig. 5C). The incision mainly progressed toward the upstream region of the anticline axis. At the beginning of this stage, candidate channels proceeded to compete for bedrock incisions. Finally, the main channel was confined to the most incised channel (deepest and widest); the others were gradually abandoned. Aside from deepening action, the main channel also widened rapidly during this period (Fig. 6, XS02 and 03). The flow route of the main channel near XS04 and 05 (Fig. 6) was not yet fixed; major bedrock erosion deflected to the left bank. The sediment in the upstream region of the uplift reach (Figs. 5C and 6, XS06) was transported downstream because the riverbed elevation downstream decreased substantially.

3.4. Stage 4: 2007 to 2010 gradual return to pre-earthquake channel slope

Two main landform changes were observed in this stage. First, the main channel on the upstream side of the anticline axis was confined closer to the left bank (Fig. 6, XS04 and 05). Intense actions of incision and widening occurred in the main channel. The bedrock erosion progressed in the upstream direction and cut through the entire uplift reach (Fig. 5D). Consequently, without the obstruction of uplifted bedrock, the channel was able to transport more sediment. The channel on the downstream side of the anticline axis had allowed considerable sediment deposition that resulted in a much smoother channel (Fig. 5D). The average channel slope of this reach had returned approximately to its pre-earthquake state (slope 1~1.3%), whereas the channel elevation was ~5 m lower than before the earthquake. This finding may indicate that, although channel adjustments in the uplift reach continued, the scale of variation may be considerably lower in the near future. Unlike the confined channel of the uplift reach, the main channel on the upstream side of the uplift reach gradually migrated from the left bank to the right bank (Fig. 6, XS06). Lateral channel migration is a typical feature of an alluvial river. Nevertheless, the bedrock river may experience lateral translation in meandering channels (Finnegan and Dietrich, 2011).

Table 1
DEM and cross secion survey data adopted in this study.

Date	Method[a]	Photographic scale (approximately)	GCPs RMS/max. error
1987	Cross section survey	–	–
1999-Sep 22	Photogrammetric, C	1:12,000	1.3/2.6
1999-Dec 10	Photogrammetric, P	1:25,000	1.6/3.0
2000-Mar	Cross section survey	–	–
2000-Nov 08	Photogrammetric, I	1:25,000	1.6/3.0
2001-Nov 12	Photogrammetric, C	1:20,000	1.6/3.0
2002-Sep 16	Photogrammetric, C	1:12,000	1.7/2.9
2003-Aug 26	Photogrammetric, C	1:22,000	0.4/0.6
2004-Mar	Cross section survey	–	–
2004-Oct 03	Photogrammetric, C	1:14,000	1.2/2.2
2005-Oct 27	Photogrammetric, C	1:20,000	1.9/3.0
2007-Jan 31	Photogrammetric, C	1:20,000	1.6/3.0
2007-Dec	Cross section survey	–	–
Date	Method	Nominal flying altitude AMSL	Point density (average)
2008-Jun 10	Airborne LiDAR	1600 m	1.6 pts/m^2
2009-Jul 23	Airborne LiDAR	2500 m	1.2 pts/m^2
2010-Sep 12	Airborne LiDAR	2500 m	1.2 pts/m^2

[a] P: panchromatic photographs; C: color photographs; I: color infrared photographs.

4. Discussion

The preceding text described the rapid change and characteristics of river morphology in the uplift reach. The uplift reach was subjected to intense bedrock erosion and was cut through by the main channel with knickpoint migration over approximately a decade (1999–2010). At the end of this period, the main channel gradually returned to an aggradational state (Fig. 5). A magnitude comparable to the astonishing rate of bedrock incision in this reach is rarely reported. Huang et al. (2008) conducted an initial study of this case and addressed the phenomena of rapid bedrock erosion with limited terrain data, aerial photos, and field investigations. They concluded that the rapid bedrock incision in this case was a local condition caused by the coseismic uplifted deformation of the Chi-Chi earthquake and noted that the geological conditions of the site were vital factors for the occurrence of the rapid incision. Plucking was considered to be the dominate erosion process. Several interesting issues deserve further elaboration and in-depth discussion.

4.1. Landform evolution after coseismic uplift

The evolution of river morphology is essentially a dynamic process; it tends to attain an equilibrium state between bedrock uplift and river incision and may self-adjust in response to tectonic processes (Burbank et al., 1996). The scale and period of the adjustment depends on the manner of disturbance during the tectonic process. The downstream

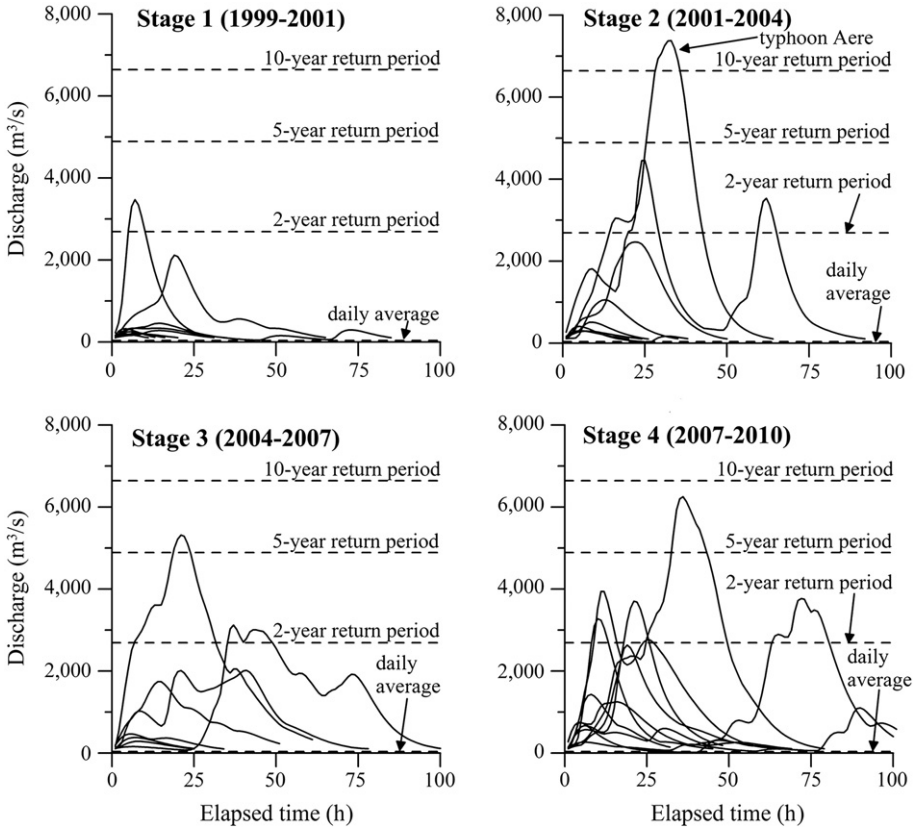

Fig. 4. Hydrographs of major floods (peak discharge >300 m^3/s) for each stage of morphology.

erosive power of river flow suddenly increased from the coseismic uplift, which triggered severe bed incision and rapid changes in landform.

The landform of the uplift reach prior to the Chi-Chi earthquake displayed a braided-type channel with a high width/depth ratio. Based on the analyses of multistaged DEM data and aerial photographs, the original thickness of the alluvial sediment was at least 3–5 m. Sudden coseismic uplift occurred in this reach. The original landform was mostly preserved, but the upper-stream rupture produced a barrier lake in its upper reach. Overtopping soon occurred because the height of the rupture scarp was only 6 m. The path of the overtopping flow followed the pre-earthquake flow channel, which was closer to the left bank (Fig. 3A). Although the landforms of the uplift reach remained relatively unchanged initially, landform evolution began to occur because the topography had changed considerably. The landform had to adapt to a new equilibrium between changing erosive power and bedrock resistance. As a result, landforms must change according to dynamic equilibrium over time (Hack, 1960).

As a result of the 10-m uplift, bedrock was greatly exposed throughout the entire wide channel in stage 1 (1999 to 2001) and was subjected to intense incision in stage 2 (2001 to 2004). A gorge-type main channel quickly formed from downstream to upstream. Various prominent landform features appeared in this reach, including narrow and deep valleys, steep cliffs, violent currents, and waterfalls at knickpoints (Figs. 3B and 7). The landforms in the uplift reach changed drastically in comparison with the wide channel prior to the earthquake. The occurrence of these landform features was largely affected by the bedrock properties and the energy of the river flow. Close observation of the landform changes revealed that channelization played an effective role in the dynamic adjustment of the river morphology from the sudden coseismic uplift.

4.2. Erosion mechanisms

Morphological changes in bedrock channels are a highly complex combination of various erosion processes, which may reflect local hydraulics, bedrock resistance/erodibility, and regional geological structures. Even within a reach, morphology in a bedrock river may exhibit high spatial variability that reflects the variability in control factors (Tinkler and Wohl, 1998). Generally, more than one process (e.g., weathering, abrasion, and plucking) may take place simultaneously; their proportions, however, are difficult to determine exactly (Whipple et al., 2000). The major erosion process was rather easily identified from field observations.

The exposed bedrock in the uplift reach was young and poorly cemented; they generally have low resistance against weathering and are particularly susceptible to cyclic wetting and drying. According to the measurements of six erosion pins installed on channel (not main channel) banks, the annual weathering depth ranged from several millimeters (for massive sandstone) to more than 100 mm (for shale). The annual weathering rate was significantly lower than the incision rate for the main channel. The upstream sediment supply was abundant; thus, abrasion by bedload saltation was expected. The notches of abrasion on the riverbed showed signs of bedload saltation (Fig. 8). Numerous field evidence indicated that erosion by plucking occurred on the main channel and its banks. Fig. 7 displays the eroded remnant of bedrock in the main channel. A comparison of the erosion scales for various erosion mechanisms indicated that plucking was likely the main contribution to erosion within the studied reach.

Plucking is often the dominant erosion mechanism in the riverbed of a heavily jointed rock mass. Because of the tectonic process and coseismic deformation, weaker rocks (e.g., shale, thin interlayer of shale and sandstone) in this reach were squeezed, whereas harder rocks (e.g., layered or massive sandstone) were overstressed and fractured (Fig. 9). Surficial flat fragments or small pieces of shale and thin interlayered shale/sandstone were easily removed by river flow (Fig. 10A). Moreover, broken sandstone blocks that were as large as a meter may lose support and stability after the underlying weaker rock layer is eroded (Fig. 10B). Relative to weathering and abrasion, plucking of rock blocks was the most effective process for large quantities of bedrock erosion in a short time. Joint spacing in this reach was generally in the scale of submeters. Erosion by plucking was common in the uplift reach. Therefore, plucking was considered the dominant erosion mechanism in the reach.

The orientation of bedrock with respect to the direction of flow also showed strong influence on the erosion process in the area adjacent to the knickpoints. Because of the existence of the Tungshih anticline, three types of rock beds based on bedding orientation with respect to flow direction were classified in this reach (Fig. 2). The three classes are dip rocks, horizontal rocks, and reverse rocks.

For the channel on dip rocks, the knickpoints were formed parallel to the bedding planes. Occasionally, a scour hole developed in front of the knickpoints because of large head differences. As the scour hole grew deeper and larger, the steep face of the knickpoint became unstable and slid down because of plane failure (Fig. 11A). For the channel on horizontal rocks, a uniform incision along the bedding planes was noticeable. The harder top layer, if it remained intact, protected the underlying softer layer. As long as the incision cut through a harder layer (e.g., neighboring potholes interconnected into flutes and then progressively deepened and expanded into a channel), the knickpoint often formed at the endpoint of a hard rock layer with a sudden drop in base elevation (Fig. 11B). The scouring of the underlying weaker layer promoted the plucking of the overlying harder layer and hence accelerated the erosion rate for the horizontal rocks. For the channel on the reverse rocks, the erosion process was controlled by the weaker layer in the rocks. Once the weaker layer was eroded and removed, the harder layer became overhung and unstable; plucking consequently ensued (Fig. 11C).

4.3. Knickpoint retreat—the primary reason for rapid incision

From worldwide erosion data (Tinkler and Wohl, 1998; Stock et al., 2005), the long-term incision rate for bedrock channels usually ranges from millimeters to submillimeters per year. Yet, the short-term incision is possible to occur as much as hundreds of millimeters. Based on incision-rate data of Taiwan, the denudation rate in the Taan River was ~2 mm/year (Li, 1976). In the western foothills of Taiwan, the decadal-scale erosion rates calculated from fluvial suspended sediment observations increased to 60 mm/year (Dadson et al., 2003). The reach-scale river incision rates (determined via dating by ^{14}C) exceeded 15 mm/year (Hsieh and Knuepfer, 2001). Short-term erosion rates that were measured by erosion pins at the upstream of the Che-Long-Pu fault scrap were >125 mm/year (Stock et al., 2005). Based on GPS data, the regional post-seismic vertical displacement around the study reach was ~144 mm (Yu et al., 2003). In comparison with worldwide data, either the long-term or short-term incision rate in Taiwan was already high relative to other regions in the world; yet the meter-scale incision rate that occurred in the studied reach was two orders of magnitude higher. The main reason for this rapid and severe channel incision was the coseismic uplift during the 1999 Chi-Chi earthquake. Possible reasons for the unusually high rate of bedrock incision were subsequently discussed further along with the topographic data of channel evolution.

Fig. 12 displays the chronological longitudinal cross sections along the main channel (the location indicated in Fig. 3). Noting the variations in terrain during consecutive years, two main forms of riverbed

Fig. 5. Longitudinal geological profiles of the main channel (strata adopt the color usage in Fig. 2): (A) Stage 1: 1999 to 2001; (B) Stage 2: 2001 to 2004; (C) Stage 3: 2004 to 2007; (D) Stage 4: 2007 to 2010. Numbers 02–06 are the locations of lateral cross sections in Fig. 6. Major transformative locations (ruptures, hinge of anticline limbs, and anticline axis) are also marked on the profiles. The vertical scale in the profiles is exaggerated 10 times.

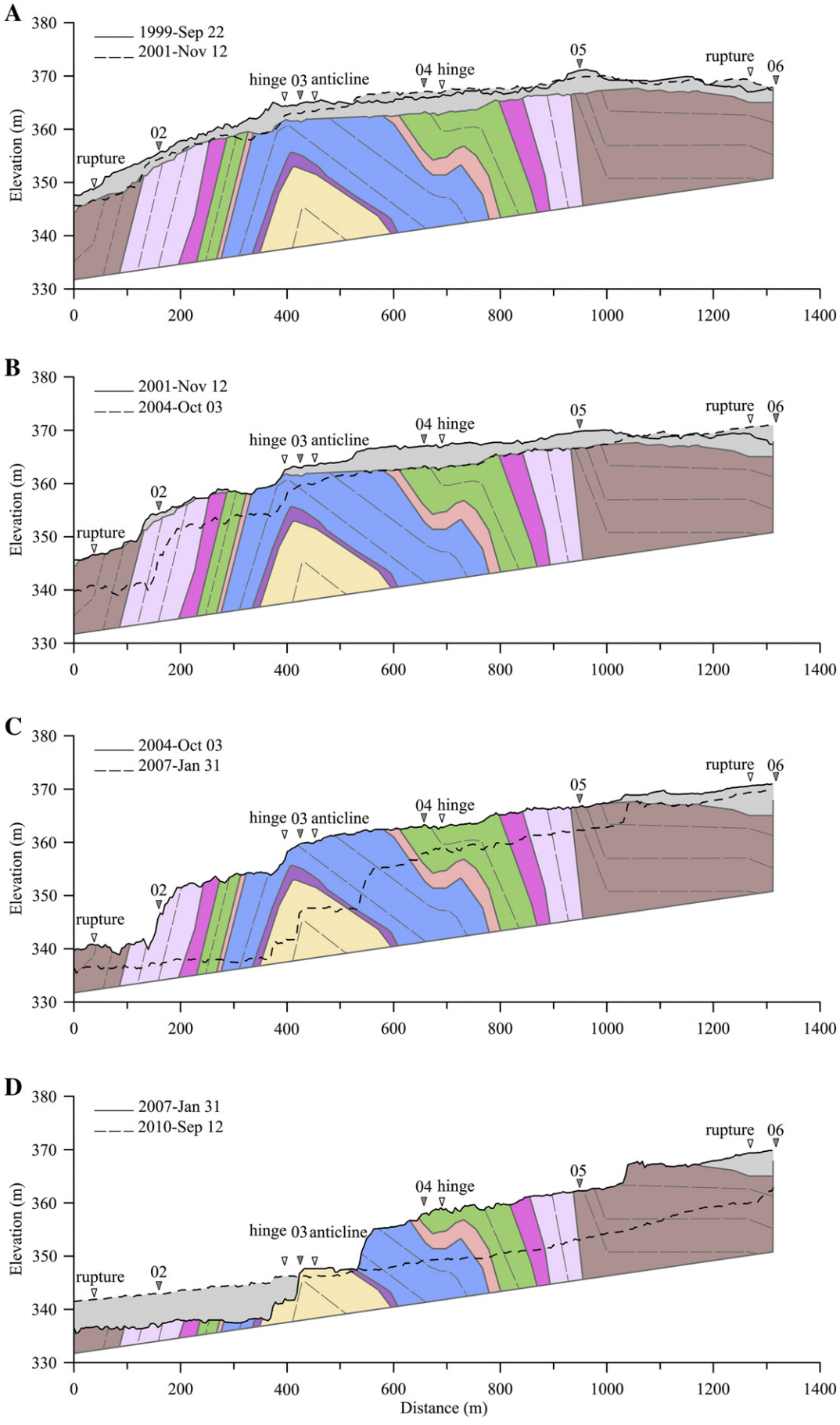
A
1999-Sep 22
2001-Nov 12
hinge 03 anticline
04 hinge
05
rupture
06
02
rupture
B
2001-Nov 12
2004-Oct 03
hinge 03 anticline
04 hinge
05
rupture
06
02
rupture
C
2004-Oct 03
2007-Jan 31
hinge 03 anticline
04 hinge
05
rupture
06
02
rupture
D
2007-Jan 31
2010-Sep 12
hinge 03 anticline
04 hinge
05
rupture
06
02
rupture
Elevation (m)
Distance (m)
380
370
360
350
340
330
0
200
400
600
800
1000
1200
1400

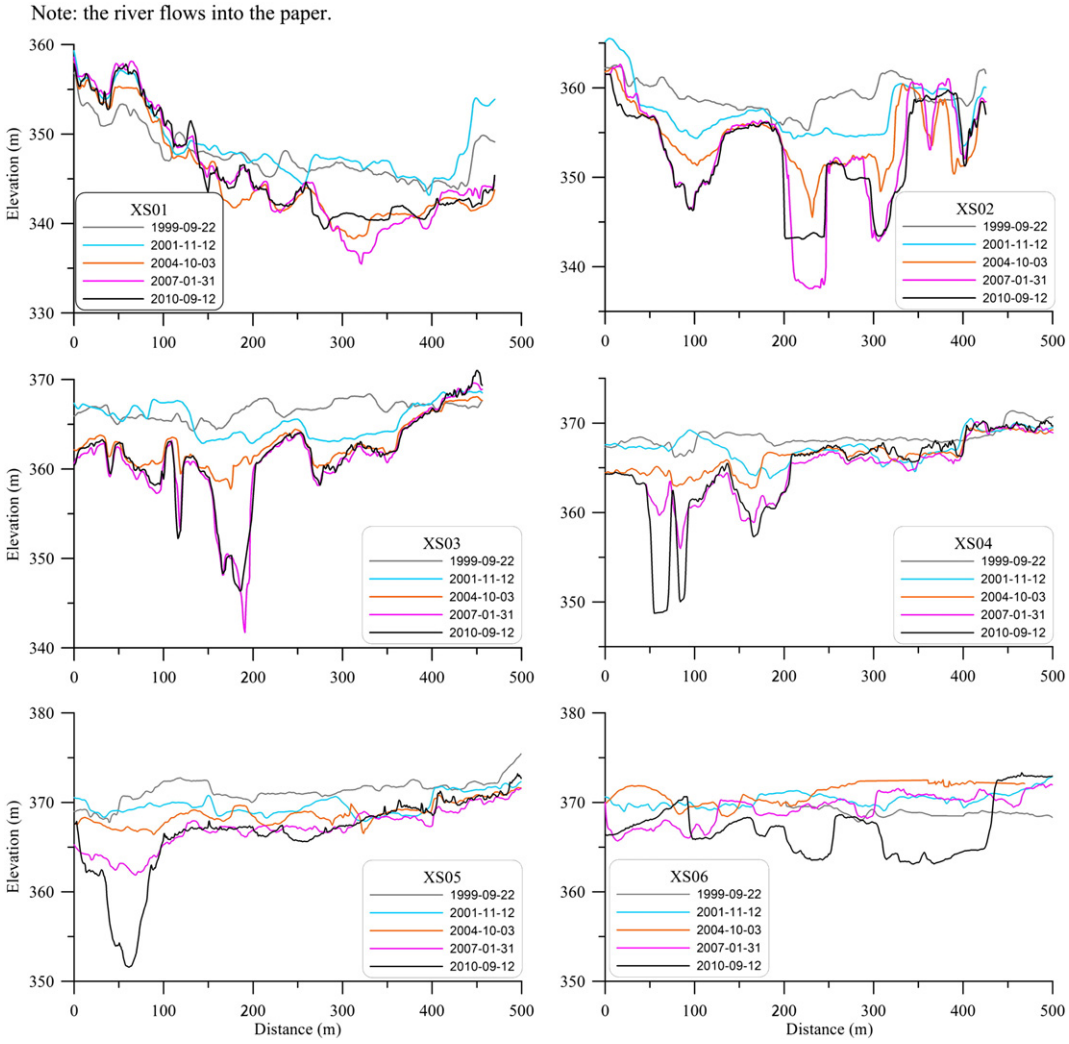

Fig. 6. Lateral (i.e., perpendicular to the flow direction) cross sections in each stage of river morphology. The locations of lateral cross sections are indicated in Figs. 1E, 3, and 5. The vertical scale in the cross sections is exaggerated 10 times. Note that stage 1 was during 1999 and 2001, stage 2 was during 2001 and 2004, stage 3 was during 2004 and 2007, and stage 4 was during 2007 and 2010.

shaping actions were observed. First, after the disappearance of the armor layer, the riverbed was subjected to a uniform incision as discussed in the preceding text (Fig. 5). The other action was associated with the development of the main channel and involved the phenomena of KPR and inner-gorge widening. Two main knickpoints, KP1 and KP2, appeared in this reach (Fig. 12, KP1 and KP2 are marked as squares and triangles, respectively). Knickpoint 1 was formed on the downstream side of the uplift rupture scarp, whereas KP2 was formed at the hinge of the anticline axis near the downstream limb (Huang et al., 2012). Three types of knickpoint retreats were discussed by Huang et al. (2012): (i) knickpoint in dip rocks, (ii) knickpoint in horizontal rocks, and (iii) knickpoint in reverse rocks. These types of knickpoint retreats are not fully consistent with common models of knickpoint evolution (Frankel et al., 2007), but are rather similar to their combinations.

Several interesting findings are associated with the phenomena of knickpoint retreat in this uplift reach. Both KP1 and KP2 formed on the wide channel after the Chi-Chi earthquake (Fig. 12). The knickpoints did not retreat for the first few years until the main channel was gradually formed in stage 2 (2001–2004). After the formation of a deep and narrow channel, the flow became more concentrated with higher stream power. Once the stream power exceeded the threshold to trigger KPR (Crosby and Whipple, 2006), KPR gained control over the channel incision.

The annual (vertical) incision ranged from 2 to 14 m for KP1 and from 2 to 11 m for KP2. The variation trend of the incision rates consisted of increasing to a maximum and then decreasing. The incision rate upstream of knickpoints was away from the influence of KPR; it was merely a flat bottom incision (FBI). The annual FBI rate ranged from 2 to 6 m upstream of KP1 and from 2 to 4 m upstream of KP2. The maximum incision rate at KP1 was higher than the maximum incision rate at KP2 because KP1 was on the downstream side of KP2, which was affected by the increase in stream power. The annual migration distance ranged from 50 to 180 m for KP1 and 60 to 350 m for KP2. The annual migration distance varied up to 6 times and was likely affected by the flood magnitude. Nevertheless, the rate of KPR was strongly affected by the erosion mechanisms associated with the geological conditions.

Compared with the incision rates associated with KPR and FBI, the incision rate associated with KPR was at least 1.5 times the incision rate for FBI. The maximum ratio of the incision rate associated with KPR to the incision rate associated with FBI was almost 6 (Fig. 12). Hence, rapid KPR appeared to be the primary reason for the unusually high rate of bedrock incision in this reach.

Fig. 7. The gorge-like channel with steep cliff banks. A branch in the left side created a knickpoint near the junction. For reference, the height of the wood pillar fence is 1 m.

Fig. 8. A massive sandstone preserved the notches of abrasion by bedload saltation.

4.4. Evolution features of the main channel

Summarizing the morphological changes in each stage, the main channel was formed in the following sequences. It was gradually formed after competition by candidate channels. With the river flow concentrated in the main channel, the knickpoint migration initiated and promoted severe incision. The banks of the main channel were unstable because of toe scouring and began to widen. In the XS02 and 03 regions (Fig. 6), the main channel formed in stage 2 (2001–2004), intensely incised in stage 3 (2004–2007), and gradually widened in stage 4 (2007–2010). Similar sequences also occurred in the XS04 and 05 regions (Fig. 6). The main channel formed in stage 3 (2004–2007) and intensely incised in stage 4 (2007–2010). The main channel was expected to widen gradually afterward.

Regarding the longitudinal profile, the average slope of the main channel in this reach returned to pre-earthquake state. This occurrence was coincident with the period in which the rapid KPR cut through the entire uplift reach. After the disappearance of knickpoints, the erosion and sedimentation gradually reached an equilibrium state. The main channel should have gradually arrived at a relatively stable state. Without new large disturbances from further tectonic processes, further severe channel incision should not occur in the future.

The strike of the rock strata in this reach was generally perpendicular to the approximate flow direction. The cliff banks in the main channel were steep. Because of the weakness and abundant fractures of the bedrocks, toe scouring of the river bank was rather common and resulted in the instability and collapse of the overlying rock, which may promote widening action in the channel (Fig. 7). Regarding the long-term evolution of the main channel, the adjustment in channel width was likely the primary change of landform. The widening action of the channel effectively reduced the stream power of flow in the channel; it lowered the chances of flow concentration and excess incision. As aforementioned, KPR cut through the uplift reach; in cases of a flood with a long returning period, the stream power will mainly accelerate the widening action of the channel instead of inducing rapid incision. The widening process in the long term may gradually erode the majority of the uplifted earth material.

Simon and Rinaldi (2006) and Yanites et al. (2010a) proposed models to describe channel evolution in response to a disturbance by tectonic process for riverbed geomaterials of cohesive soil and bedrock. Their models have some common features. The extra stream power, because of a sudden rise in the base level of erosion, caused channel incision. After the channel was deepened, the channel banks became unstable and began widening. Along with channel widening, the stream power decreased gradually; eventually sediment deposition reactivated.

4.5. Impact of the uplift on the Taan River

Before the 1999 Chi-Chi earthquake, the Taan River was a typical graded stream with a smooth longitudinal profile (Fig. 13, 1987 profile). The coseismic uplift disturbed the original equilibrium state of the river system; it caused deposition upstream and incision downstream. The affected region in the river is ~5 km (Fig. 13, distance 24,500–29,500 m). Because of the bedrock incision in this reach for approximately a decade,

Fig. 9. Heavily jointed rock masses arise from coseismic uplift. (A) The anticline axis and the hinge of the west limb. (B) Horizontal rocks near the anticline axis. For reference, the height of the wood pillar fence is 1 m.

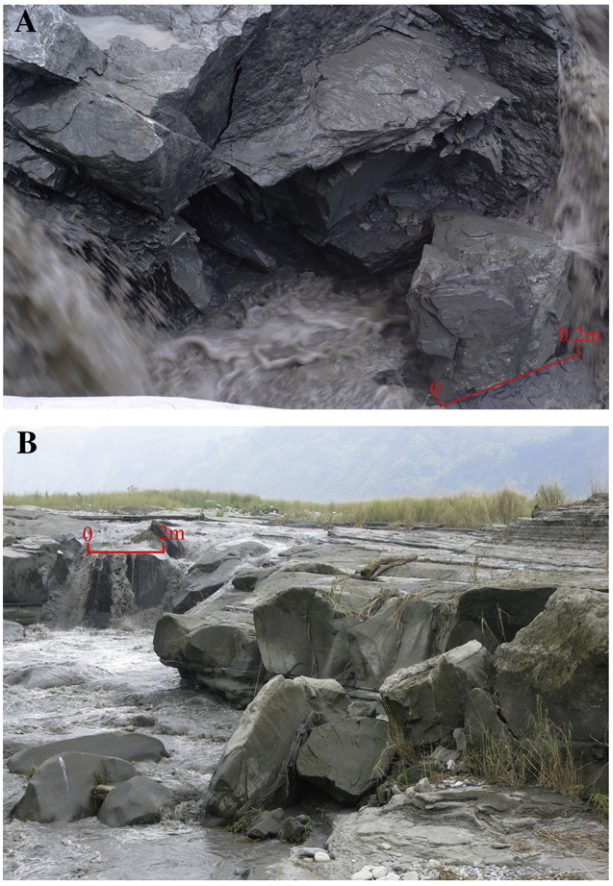

Fig. 10. Plucking process in the reach on (A) interlayered shale and sandstone; (B) massive sandstone.

a gorge-type channel formed and carved through the entire uplift reach; afterward, deposition gradually returned. The reach gradually returned to the original average slope.

At the beginning of the channel-carving process, upstream sediments were blocked by the uplift and could not transport downstream; together with the channel incision, the base elevation in the downstream decreased gradually. Compared with a maximum uplift of 10 m, the maximum depth of incision was ~20 m and revealed excess incision. Three reasons were for the excess incision. First, the sediment supply from upstream was reduced. Second, flow concentration in narrow valleys increased the stream power. Third, the elevated stream power at the knickpoints generated scour holes and contributed to the excess incision. However, after the main channel cut through the uplift reach, the sediment supply returned, sediment deposition was reactivated (the sedimentation thickness was 4–6 m in the downstream channel as shown in Fig. 5D), and the excess incision gradually reduced.

Besides the influence of coseismic uplift, the imbalance of sediment transport was also affected by the dredging operation after the earthquake. The dredging operation affected the uplift reach in two aspects. First, it advanced the exposed time of the rock bed and subsequent rock erosion. Next, the operation attempted to divert the flow route from closer to the left bank to closer to the river center. Fig. 3 shows that the natural flow route after the earthquake (but before dredging) was consistent with the final main channel. The influence of flow route diversion by man-made dredging only had a temporary effect. The channel evolution was eventually dominated by factors of channel morphology and geology.

As shown in Fig. 13, the range of river affected severely by the uplift was a total of 5 km: 1 km in the uplift reach and 4 km in the downstream reach. The reason for a longer affected range in the downstream

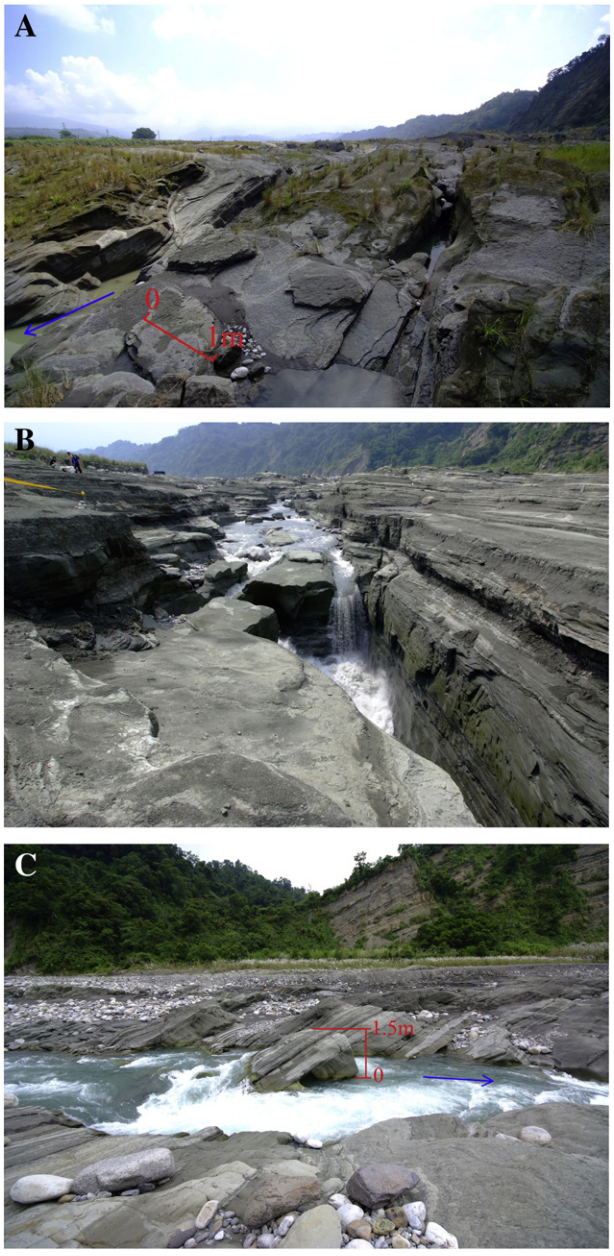

Fig. 11. Influence of bedding orientation on riverbed incision for (A) dip rocks; (B) horizontal rocks (the people in upper-left are for scale reference); and (C) reverse rocks. The arrow indicates flow direction.

reach was that upstream sediment supply was not able to fully transport downstream and stream power increased. The Cholan bridge was located 2 km downstream of the uplift reach. The bed erosion adjacent to the Cholan bridge was caused by local scour as well as excess incision from the existence of KP1. It resulted in the exposure of the bridge pier, which led to bridge damage.

As indicated by erosion downstream of the uplift reach, stream power raised by the uplift could not quickly dissipate after the flow left the reach. The elevated flow energy could transport extra sediments to the downstream hence had a higher erosive power to erode the downstream riverbed. From the profiles in Fig. 13, the extra stream energy was most likely fully consumed downstream after 4 km. It reflects the fact that the impact of the coseismic uplift in 1999 on the Taan River was a local incident affecting a total length of 5 km. The affected zone was not long in terms of the scale of the entire catchment. However, from an engineering point-of-view, the equilibrium of the local fluvial reach was largely disturbed. It certainly had a severe impact on channel morphology and

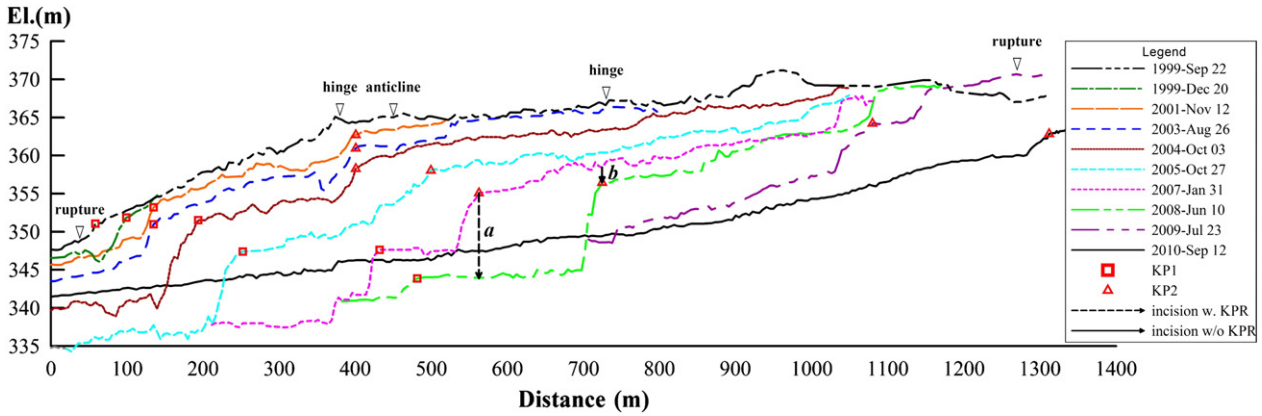

Fig. 12. Chronological longitudinal profiles along a deep channel within the uplift reach (modified from Huang et al., 2012). The maximum ratio of incision with KPR over incision without KPR = $a/b = 5.7$; the magnitudes of a and b are indicated by the dash arrow line and the solid arrow line, respectively.

seriously threatened the stability of all infrastructures across the river channel within the affected reach. The damage to the piers of the Cholan Bridge was a real example.

5. Conclusions

The coseismic deformation in the Chi-Chi earthquake produced fault scarps and a pop-up structure across the Taan River. The maximum vertical slip of the fault scarps, which was ~10 m, disturbed the dynamic equilibrium of the fluvial system; as a result, severe rapid incision of weak bedrock was activated after its armor layer was removed. The maximum incision rate was 14 m/year; whereas the maximum annual rate of KPR reached 350 m. This work adopted the uplift reach as a case study to closely observe and record the progressive evolution of river morphology subjected to sudden uplift. Based on multistaged orthophotographs and DEM data, the process of morphology evolution in the uplift reach was divided into four distinct stages: (i) loss of armor materials, (ii) intense incision of exposed bedrock, (iii) formation of the main channel, and (iv) gradual return to the pre-earthquake channel slope.

Notable landform features in this reach (e.g., narrow and deep valleys, steep cliffs, violent currents, and waterfalls at knickpoints) were the result of dynamic adaption of the river in response to the sudden uplift. Discernible erosion mechanisms in this reach were identified. Plucking was the dominant erosion mechanism associated with channel incision and knickpoint migration. The rate of KPR was affected by factors including discharge, rock properties, geological structures, and bedrock orientation. The unusually high rate of KPR may have been responsible for the rapid incision in the main channel. The channel slope recovered to the pre-earthquake state because the main channel cut through the uplift reach. Additional large floods are expected to cause significant widening of the channel instead of inducing more incision. The total length of the river reach affected severely by the coseismic uplift was ~5 km: 1 km in its uplift reach and 4 km in its downstream reach. The downstream reach was affected because of the reduction in sediment supply and the increase in stream power. Although the affected zone was short in terms of the scale of the entire

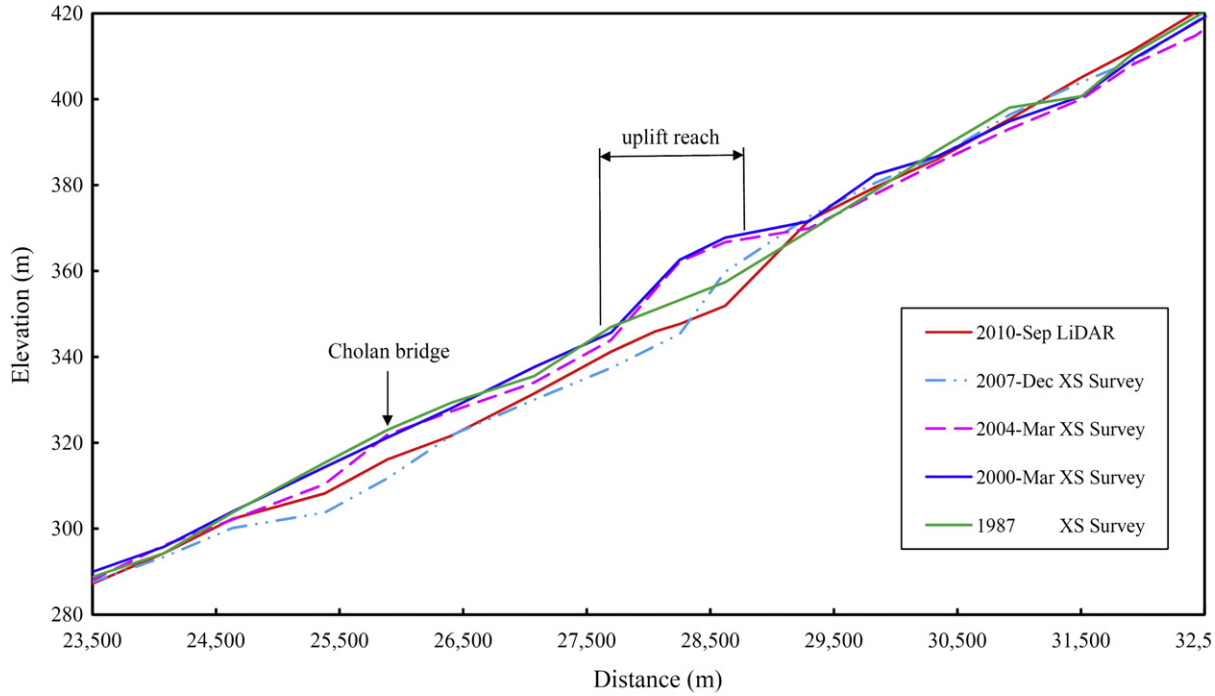

Fig. 13. The chronological longitudinal profiles between 23,500 and 32,500 m from the estuary. These profiles, in consecutive periods, show the multistaged variations of incision/deposition from upstream to downstream of the uplift reach.

catchment, its occurrence may seriously threaten the stability of the infrastructures across the river channel within the affected zone.

Acknowledgements

The work presented in this paper was made possible through the support of the Water Resources Planning Institute, Water Resources Agency, Ministry of Economic Affairs, Taiwan, and the National Science Council (Project nos. 98-2221-E-009-149-MY3 and 98-2221-E-009-152-MY3). The authors appreciate very much the precious comments from the anonymous reviewers and the editor, Prof. Richard A. Marston. Their comments made the quality of this paper significantly improved.

References

Anders, N.S., Seijmonsbergen, A.C., Bouten, W., 2009. Modelling channel incision and alpine hillslope development using laser altimetry data. Geomorphology 113, 35–46.
Burbank, D.W., Leland, J., Fielding, E., Anderson, R.S., Brozovic, N., Reid, M.R., Duncan, C., 1996. Bedrock incision, rock uplift and threshold hillslopes in the northwestern Himalayas. Nature 379, 505–510.
Chen, Y.G., Lai, K.Y., Lee, Y.H., Suppe, J., Chen, W.S., Lin, Y.N.N., Wang, Y., Hung, J.H., Kuo, Y.T., 2007. Coseismic fold scarps and their kinematic behavior in the 1999 Chi-Chi earthquake Taiwan. Journal of Geophysical Research-Solid Earth 112, B03S02 http://dx.doi.org/10.1029/2006JB004388.
Crosby, B.T., Whipple, K.X., 2006. Knickpoint initiation and distribution within fluvial networks: 236 waterfalls in the Waipaoa River, North Island, New Zealand. Geomorphology 82, 16–38.
Dadson, S.J., Hovius, N., Chen, H., Dade, W.B., Hsieh, M.L., Willett, S.D., Hu, J.C., Horng, M.J., Chen, M.C., Stark, C.P., Lague, D., Lin, J.C., 2003. Links between erosion, runoff variability and seismicity in the Taiwan orogen. Nature 426, 648–651.
Finnegan, N.J., Dietrich, W.E., 2011. Episodic bedrock strath terrace formation due to meander migration and cutoff. Geology 39, 143–146.
Frankel, K.L., Pazzaglia, F.J., Vaughn, J.D., 2007. Knickpoint evolution in a vertically bedded substrate, upstream-dipping terraces, and Atlantic slope bedrock channels. Geological Society of America Bulletin 119, 476–486.
Gilbert, G.K., 1877. Report on the Geology of Henry Mountain, Utah. U.S. Geographical and Geological Survey of the Rocky Mountain Region. U.S. Government Printing Office, Washington, DC.
Hack, J.T., 1960. Interpretation of erosional topography in humid temperate regions. American Journal of Science 258-A, 80–97.
Howard, A.D., Dietrich, W.E., Seidl, M.A., 1994. Modeling fluvial erosion on regional to continental scales. Journal of Geophysical Research-Solid Earth 99, 13971–13986.
Hsieh, M.L., Knuepfer, P.L.K., 2001. Middle-late Holocene river terraces in the Erhjen River basin, southwestern Taiwan — implications of river response to climate change and active tectonic uplift. Geomorphology 38, 337–372.
Huang, M.W., Cheng, M.H., Liao, J.J., Pan, Y.W., 2008. Rapid bedrock erosion in the Taan River, Taiwan. Fourth International Conference on Scour and Erosion. The Japanese Geotechnical Society, Tokyo, Japan, pp. 361–366.
Huang, M.W., Pan, Y.W., Liao, J.J., Cheng, M.H., 2012. Knickpoint evolution across anticline structure: a case of uplift reach in the Taan River, Taiwan. Sixth International Conference on Scour and Erosion. Societe Hydrotechnique de France, Paris, France, pp. 503–510.
Lai, Y.G., Greimann, B.P., Wu, K.W., 2011. Soft bedrock erosion modeling with a two-dimensional depth-averaged model. Journal of Hydraulic Engineering ASCE 137, 804–814.
Lee, K.T., Yen, B.C., 1997. Geomorphology and kinematic-wave-based hydrograph derivation. Journal of Hydraulic Engineering ASCE 123, 73–80.
Lee, Y.H., Hsieh, M.L., Lu, S.D., Shih, T.S., Wu, W.Y., Sugiyama, Y., Azuma, T., Kariya, Y., 2003. Slip vectors of the surface rupture of the 1999 Chi-Chi earthquake, western Taiwan. Journal of Structural Geology 25, 1917–1931.
Lee, Y.H., Lu, S.T., Shih, T.S., Hsieh, M.L., Wu, W.Y., 2005. Structures associated with the northern end of the 1999 Chi-Chi earthquake rupture, Central Taiwan: implications for seismic-hazard assessment. Bulletin of the Seismological Society of America 95, 471–485.
Li, Y.H., 1976. Denudation of Taiwan island since Pliocene epoch. Geology 4, 105–108.
Liao, C.T., Yeh, K.C., Huang, M.W., 2011. Modelling of bedrock river evolution. 34th IAHR World Congress. Brisbane, Australia, pp. 4459–4467.
Loget, N., Van Den Driessche, J., 2009. Wave train model for knickpoint migration. Geomorphology 106, 376–382.
Schumm, S.A., 1979. Geomorphic thresholds — concept and its applications. Transactions of the Institute of British Geographers 4, 485–515.
Simon, A., Rinaldi, M., 2006. Disturbance, stream incision, and channel evolution: the roles of excess transport capacity and boundary materials in controlling channel response. Geomorphology 79, 361–383.
Stock, J.D., Montgomery, D.R., Collins, B.D., Dietrich, W.E., Sklar, L., 2005. Field measurements of incision rates following bedrock exposure: implications for process controls on the long profiles of valleys cut by rivers and debris flows. Geological Society of America Bulletin 117, 174–194.
Tinkler, K.J., Wohl, E.E., 1998. A primer on bedrock channels. In: Tinkler, K.J., Wohl, E.E. (Eds.), River Over Rock: Fluvial Processes in Bedrock Channels. American Geophysical Union, Washington, DC, pp. 1–18.
Tomkin, J.H., Brandon, M.T., Pazzaglia, F.J., Barbour, J.R., Willett, S.D., 2003. Quantitative testing of bedrock incision models for the Clearwater River, NW Washington state. Journal of Geophysical Research-Solid Earth 108, 19 http://dx.doi.org/10.1029/2001JB000862.
Whipple, K.X., 2004. Bedrock rivers and the geomorphology of active orogens. Annual Review of Earth and Planetary Sciences 32, 151–185.
Whipple, K.X., Hancock, G.S., Anderson, R.S., 2000. River incision into bedrock: mechanics and relative efficacy of plucking, abrasion, and cavitation. Geological Society of America Bulletin 112, 490–503.
WRA (Water Resources Agency), 2010. Report on Review of Taan River Planning. Ministry of Economic Affairs, Taipei. (304 pp. in Chinese).
Yanites, B.J., Tucker, G.E., Mueller, K.J., Chen, Y.G., 2010a. How rivers react to large earthquakes: evidence from central Taiwan. Geology 38, 639–642.
Yanites, B.J., Tucker, G.E., Mueller, K.J., Chen, Y.G., Wilcox, T., Huang, S.Y., Shi, K.W., 2010b. Incision and channel morphology across active structures along the Peikang River, central Taiwan: implications for the importance of channel width. Geological Society of America Bulletin 122, 1192–1208.
Yu, S.B., Hsu, Y.J., Kuo, L.C., Chen, H.Y., Liu, C.C., 2003. GPS measurement of postseismic deformation following the 1999 Chi-Chi, Taiwan, earthquake. Journal of Geophysical Research-Solid Earth 108 http://dx.doi.org/10.1029/2003JB002396.